An Automated Torsion Balance for Investigation of Microstructure of Single Filaments. I. Polypropylene

MARIAN GAYLE MCCORD* and MICHAEL S. ELLISON†

School of Textiles, Fiber, and Polymer Science, Clemson University, Clemson, South Carolina 29634-1307

SYNOPSIS

The tensile properties of filaments have been related to fiber microstructure in numerous studies over several decades. However, there have been relatively few attempts to relate shear modulus to microstructure: most of the work on shear properties of filaments was done over 20 years ago. Since then, there have been advances in instrumentation and polymer technology. We present a review of the literature in these areas. We report the construction of a fully automated torsion balance and its efficacy in an investigation of the relationship between polypropylene (PP) fiber microstructure and shear modulus. This work lays the foundation for a definitive research program into microstructure/shear properties' interrelationships in fibers. Our torsion test apparatus is an enhanced implementation of the simple torsion balance. Data acquisition and test parameters are completely controlled by a microcomputer. Raw data from digital position encoders is converted into torque–twist data, which is then presented to a statistical program to determine the initial shear modulus of the filament. Torsion testing was performed on six PP fiber samples. It was found that the shear modulus of the filaments increased with an increase in amorphous orientation, but that in a filament with a radially differentiated structure, the relationship is biased by the modulus of the outer portion of the filament. © 1996 John Wiley & Sons, Inc.

INTRODUCTION

Mechanical properties of fibers are typically investigated through a variety of physical testing techniques in which tensile deformation is employed, while relatively few studies have addressed the shear properties of fibers. Investigations of the shear properties of fibers were conducted as early as the 1920s, when Peirce reported on the mechanical properties of cottons.[1] There was a small but steady continuation of this work until the mid-1970s. After a hiatus of nearly a decade, DeTeresa et al. rekindled interest in fiber shear properties.[2]

A state of shear in a cylinder is most easily accomplished by twisting (torsion). Although knowledge of fiber shear properties is essential for a comprehensive analysis of typical textile operations such as yarn formation, twisting, and texturing, the real significance of these properties may be in their relationship to and indication of fiber microstructure.

A simple and popular method for determination of the shear modulus is the simple torsion pendulum, in which an inertial mass suspended by a filament is allowed to oscillate freely after a small initial displacement. The decaying amplitude of oscillation may be used to determine the damping constant of the filament and the frequency of oscillation is inversely related to the shear modulus of the filament.[3-14]

Frequency limitations of the free torsion pendulum have been overcome by the use of forced oscillations. Wakelin and colleagues used the electrostatic vibroscope to measure the shear modulus of nylon 6,6 and Dacron® filaments at frequencies up to 437 Hz.[15] Nordon employed a magnetic, rather than electric, method of inserting twist, in the range of 1–200 Hz.[16,17] Neither of these techniques allows for significant increases in strain over the simple torsion pendulum.

* Present address: College of Textiles, Box 8301, North Carolina State University, Raleigh, NC 27695-8301.

† To whom correspondence should be addressed.

Journal of Applied Polymer Science, Vol. 61, 293–306 (1996)
 CCC 0021-8995/96/020293-14

The torsion balance provides a wide range of both strain rate and amplitude. An element of known shear modulus, typically a wire, is connected to a fiber via a rigid shaft. Twisting the fiber results in displacement of the wire. A sensor located on the shaft indicates the amount of twist in the wire, and from this information, the torque exerted by the fiber on the wire can be calculated. Knowledge of this torque permits a determination of the shear modulus of the fiber.[1,18–27] Our instrument is an enhanced implementation of this basic design.

Shear Behavior of Fibers

There are relatively few studies that examine the relationship between shear modulus, or a related property, and fiber structure. Most earlier work was performed on natural fibers.[1,9,12,13,16–18] This review addresses the instrumentation and studies on synthetic fibers exclusively.

Studies of the relationship between torque and twist in yarns were performed by Peirce in 1923 and by Steinberger in 1936.[1,28] In 1949, Morton and Permanyer adapted the torsion balance to make it suitable for testing single fibers.[25] Using this apparatus, they reported measurements of torque/(cross-sectional area)^2 on viscose rayon, Tenasco, acetate, and nylon filament. The filaments ranged in denier from 3.0 to 4.75.

The relationship between shear modulus and orientation in filaments has been investigated, but the reports are conflicting. Pioneering work by Meredith reported on the use of a simple torsion pendulum to determine the shear moduli of a large variety of textile fibers.[10] He reported that the ratio of tensile modulus to shear modulus (E/G) appeared to be related to fiber anisotropy. Confirmation of this theory was provided by Wakelin et al. in a study of the torsion moduli of nylon 6, 6 and Dacron.[15] It was found that upon increasing the draw ratio of these filaments, E/G increased substantially. This effect was attributed solely to the increase in tensile modulus with draw ratio. While the authors proposed that there was no significant effect of drawing on the shear modulus of nylon 6, 6 or Dacron, we conducted a closer examination of their data that revealed that there is a slight increasing trend in shear modulus with draw for nylon 6, 6 and for Dacron. Nevertheless, it is evident from this data that the drawing process affects the tensile modulus to a much greater extent than it does the shear modulus. It was further proposed by those authors that the primary effect of drawing was located in the center, or core, of a filament, while the outer region remained mostly unchanged.[15] Processing conditions were not provided.

Guthrie et al. reported on the torsional rigidity of several synthetic filaments.[8] The authors claimed that the torsional rigidity was higher for fibers with a typically lower orientation than for those with a higher orientation. However, they did not report the actual draw ratio or birefringence of their fibers, relying instead on generalities such as higher tenacity and lower extensibility as an indication of orientation.

Mertens measured the torque in nylon 6 filaments with a torsion balance.[23] The cold drawn nylon 6 filaments had a range of orientation as indicated by birefringence values from $\Delta n = 0.043$–0.054. Another set of filaments were heat treated under tension for a brief period (0.5–3 s) in a hot air oven. Birefringence values for these filaments ranged from 0.047 to 0.058. Mertens found that the slope of the torque versus twist curve increased with birefringence in both the cold-drawn and heat-set filaments.

The issue of nonuniform cross-sectional microstructure was addressed by Owen, who measured bending and torsional rigidity of natural and synthetic filaments.[12] Owen proposed that the ratio of these quantities was an indicator of fiber anisotropy, hence, orientation, and that, in a structure with a pronounced skin–core structure, the ratio would be biased toward the values of the skin region.

Hadley and coworkers measured the independent elastic constants (assuming transverse isotropy) for five synthetic filaments: low density polyethylene (PE), high density PE, nylon 6, 6, polyethylene terephthalate (PET), and polypropylene (PP).[29] Torsional modulus was determined by means of a simple torsion pendulum, similar to that used by Meredith.[10] The effect on the torsional modulus of changes in draw ratio varied among the different types of filament. In their work, the shear modulus of low density PE and PET dropped with an increase in draw ratio; the opposite occurred for PP and, to a lesser extent, for high density PE. For the nylon filaments, there was an initial maxima at a low draw ratio, followed by a steep drop at a slightly higher draw ratio.

Dhingra and Postle studied the torsion of nylon 6 monofilament.[19,20] The torque twist curve of the monofilament indicated a gradual onset of yielding. At high levels of twist, the curve began to rise sharply, indicative of a strain hardening process. The response of the filament appeared to be independent of the rate of twisting. The torsional modulus decreased with an increase in filament diameter. Diameters ranged from 160 μm to 1.1 mm.

The most recent work is that of Zeronian et al. in which a torsion pendulum was used in a study on the interrelationships between fiber properties.[30]

PP Filament

PP solidified from a quiescent melt typically forms a spherulitic monoclinic crystalline structure consisting of randomly oriented stacks of folded-chain lamellae, although high quench rates may yield well-oriented paracrystallinity or smectic crystallinity.[31,32] Both crystallization kinetics and microstructure are significantly altered by solidification under spinline stress. At very low stress levels (e.g., mass flow rate of 1.93 g/min, take-up velocity between 0 and 50 m/min), there is a transition from spherulitic to row-nucleated crystalline structure, as well as a change in the crystallization temperature and rate.[33]

For normal spinning in air, average filament temperatures reach approximately ($T_{ambient}$ + 30°C) at distances of approximately 30–100 cm from the spinnerette. There is no method for measuring radial temperature gradients in the filament during spinning. Models of the molten filament predict radial gradients on the order of 10^3–10^4°C/cm.[34] The effect of radial temperature gradients on crystalline microstructure may be significant. Crystallites tend to orient in the direction of a temperature gradient in a quiescent melt.[35] If this occurred in the spinline, there may be some distribution of these crystallites among those oriented in the direction of elongation. Another consequence of the thermal gradient is the nonuniform stress distribution in the filament, higher in the surface layers than in the center of the filament. Extreme cases of this stress distribution, typical in high-speed spinning, yield a more oriented, less crystalline "skin," and a less oriented, highly crystalline "core." Such skin–core effects may be detected using interference microscopy.

An increase in spinline stress increases the temperature at which the onset of crystallization occurs.[33] In that report, this effect was found to saturate at low levels of spinline stress due to the increased effect of cooling rate at higher take-up velocities. The temperature in the threadline decreased rapidly until the onset of crystallization, when heat liberated by crystallization resulted in a temperature plateau for a period of time during which nearly 60% of the ultimate crystallinity was achieved. Higher solidification rates led to relatively low crystallinities with high degrees of orientation, while lower rates had the opposite effect.

Drawn Filament

Formation of Microfibrillar Microstructure

The final form of an as-spun (i.e., undrawn) PP fiber consists of chain-folded crystalline lamellae, with some variation in degree of orientation, which is dependent on spinline parameters as previously discussed. The lamellae are closely packed and joined by tie molecules incorporated in two or more crystallite layers. The primary effect of drawing is to disrupt the as-spun structure and transform it to a microfibillar structure possessing much greater tensile strength and modulus, and a much lower elongation to break.[31,35,36]

The physical manifestations of drawing include the appearance, upon splitting and peeling, of fibrillation in the drawn filament, as seen in scanning electron microscopy (SEM) photographs.[37] This effect is much greater in samples with low as-spun crystalline orientation and is more severe in cold drawing than in hot drawing (drawing close to the melt temperature).[37–39] As draw ratio increases, the extent of fibrillation increases, while filament density decreases.[39] Birefringence increases with increasing amount of fibrillation, and tensile strength and modulus increase with increasing birefringence.[37,39]

The appearance of fibrillation is coincident with development of diffuse equatorial scattering in the filament small angle X-ray scattering (SAXS) pattern, indicating the presence of elongated void spaces.[37] In that work, Bodaghi and cohorts found that amounts of crystallinity of PP filaments predicted by density measurements were significantly lower than those calculated from differential scanning calorimetry (DSC) data. This discrepancy was attributed to the existence of void spaces. Cold drawing, drawing at a temperature well below the melt point of the polymer, initially results in necking at one or more points along the filament length in filaments with low initial orientation, with subsequent decrease in diameter before filament break. Highly oriented as-spun material deforms evenly without evidence of neck formation. Noncrystalline regions yield to stress first and rapidly become oriented in the direction of the stress.[40]

Microfibrils appear to aggregate in larger units known as fibrils, the boundaries of which correspond to intercrystalline regions in the as-spun lamellar material. The interfibrillar tie molecules that bind fibrils to one another are less dense than those that bind microfibrils.

Orientation

The relationship between molecular orientation and tensile modulus of melt spun fibers has been thoroughly investigated: a higher draw ratio yields a higher modulus fiber with a higher birefringence.[31-33,37-39,41,42] Increase in birefringence is a result of an increase in the axial orientation of the noncrystalline (amorphous) as well as the crystalline microstructural regions of the fiber.

Once the fibrillar structure has formed, the major effect of continued drawing is fibrillar slippage under the axial stress. Fibrils slightly inclined to the strain axis are subject to shear stress. This shear stress also leads to microfibrillar slippage, although to a much lesser extent than that of the fibrils. The tensile modulus of a drawn fiber depends upon the numbers of both inter- and intrafibrillar tie molecules and their tautness in and between fibrils and microfibrils.[36] While drawing causes an increase in the volume percentage of tie molecules by extending their folded chain segments, the extent of this increase is limited by the length of the molecules. The importance of tie molecules in fiber modulus and strength decreases with increased incidence of chain pullout from crystallites as draw ratios increase beyond a critical limit.

Crystalline orientation as measured by wide angle X-ray scattering (WAXS) increases with an increase in draw ratio and molecular weight (MW), and with a decrease in draw temperature. Crystallinity increases with increasing draw ratio and temperature but does not appear to be affected by MW. WAXS data suggests that cold drawing either changes the PP crystalline unit cell from a monoclinic to a smectic form, or creates a much smaller crystallite size, or perhaps causes a combination of these effects.[37]

Annealing

Annealing, or heat setting, of melt-spun drawn filaments primarily serves to remove residual internal stresses and to perfect crystalline order.[39] WAXS has shown that annealing at temperatures near but below the melting temperature increases the crystallite size, and when the crystallite has been disrupted, returns it to its original form.[43] If the filament is unrestrained during the annealing process, the sample shrinks as tie molecules between fibrils cause crystallite rotation in an attempt to return the microstructure to its predrawn state. This may result in a decrease in elastic modulus to close to that of the undrawn filament.[36] In samples annealed at fixed length, interfibrillar tie molecules may maintain filament length, but there is some shrinkage and reorganization within the microfibrils, as well as axial microfibril sliding. In either case, the amount of noncrystalline material decreases with heat setting.[36]

EXPERIMENTAL

Torsion Test Apparatus

While there is at least one torsion balance apparatus commercially available, it is limited to a twisting rate of 1 rpm.[26] To provide a wider operating range, a torsion test apparatus was designed and built in-house. The instrument (Fig. 1) is an enhanced implementation of the generic torsion balance introduced in the previous section. Motion control is provided by a nuLogic, Inc., nuControl® 3-Axis DC Servo Motor Control Board installed in a Macintosh® Quadra 950 computer. Pittman Corp. DC servo motors are used to insert the twist in the fiber. The motors are each equipped with 500 slot encoders. Only the bottom motor was active for the present studies. The nuControl board provides control of both motors and monitors the position of the center encoder. The output drive voltage of the board is bipolar analog with a ±5-V swing. Closed-loop control is provided by position feedback information from the quadrature encoder inputs.

A program written in LabVIEW2® software (National Instruments Corp.), which allows the user to

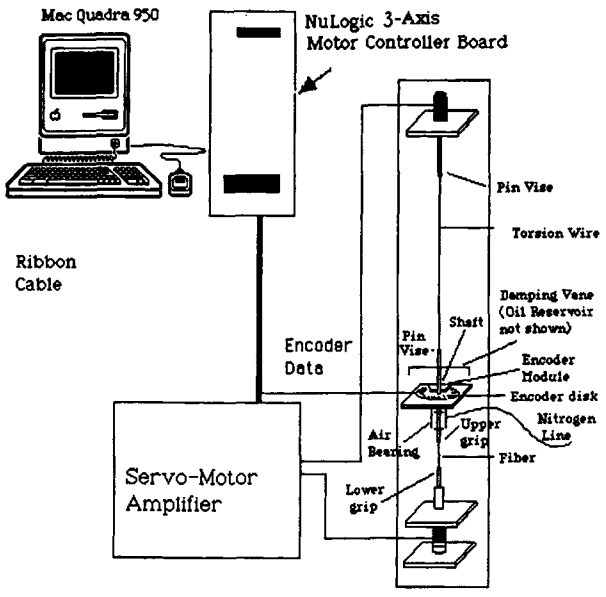

Figure 1 Schematic of a torsion test apparatus for single filaments.

program using graphic icons linked by "wires" rather than textual commands, is used for simultaneous instrument control and data acquisition. The application programs created by the user are called virtual instruments (VIs), and consist of a "front panel" and a "block diagram." The front panel is visually an instrument panel, with icons representing switches, dials, chart or strip recorders, buttons, and other elements with which the user interacts to run the program and to set up experimental conditions. The actual construction of the program takes place within the block diagram. A set of LabVIEW2 VIs specific to the nuControl board was furnished by nuLogic. These VIs provided the control and read commands for the board.

Variables include rate and time period of deformation. The torsion test program for torsional modulus data allows the user to program the number of revolutions and the speed for the bottom motor. During acquisition, the data are presented on a strip recorder onscreen and may be called to an x–y graph upon completion. Position of axis 1 and axis 3, the center encoder, are monitored throughout motor motion. Position data are loaded sequentially into an array in a spreadsheet format; and at the conclusion of data acquisition, the data are written to a text file.

A 1-cm sample is mounted in specially designed grips located in the lower portion of the apparatus. The lower grip is allowed to move vertically, providing a constant tensile load on the fiber, and allowing the fiber to contract slightly upon twisting. The fiber is coupled to a stainless steel wire by a shaft and a pin vise. Wires of various diameters may be used to alter the resistance to fiber torque, thereby altering the range of the instrument. The shaft passes through an air bearing using dry nitrogen as the lubricating fluid, which provides low friction lateral stability. Attached to the shaft is a Hewlett–Packard HEDS-9000 two-channel optical encoder module and a Hewlett–Packard HEDS-6100 1000 slot incremental code wheel disk. As the fiber is twisted by the motor shaft, the fiber generates torque against the wire and causes it to turn and to displace the code wheel. The program records code wheel motion data throughout displacement of the fiber. Position changes are recorded by the program as encoder line counts, with four counts for every encoder line, 2000 counts per revolution for the motor encoder, and 4000 counts per revolution for the middle encoder.

The torsion wire used for these PP studies was a 0.0055-in. diameter stainless steel (type 304) wire. The shear modulus of the torsion wire was calculated to be 4.8×10^{10} N/m^2 from the tensile modulus of the wire by means of the well-known relationship for isotropic solids:

$$G = E/2(1 + \nu) \tag{1}$$

where E is the experimentally determined tensile modulus and ν is the literature value of 0.30 for Poisson's ratio of stainless steel.[44] The value for tensile modulus ($1.91E3 \pm 1.9$ N/m^2) in this calculation was an average of the measured moduli of eight samples of the wire.

Data Analysis

The relationship between shear modulus and the torque T for small deformations of an isotropic cylinder (Fig. 2) is[10,44,45]

$$T = \frac{GJ\phi}{L} \tag{2}$$

where G is the shear modulus, J is the polar moment of inertia, ϕ is the rotation in radians, and L is the length.

In our torsion test apparatus, the torque produced by the fiber, T_f, is equal to the torque in the wire, T_w, to which it is coupled. Therefore,

$$T_f = T_w = \frac{G_w J_w \phi_w}{L_w} \tag{3}$$

For the fiber, the actual twist is the twist introduced by the motor at the bottom of the fiber (axis 1) minus the twist allowed by the wire and recorded by the middle encoder (axis 3). Twist is computed from position count data by

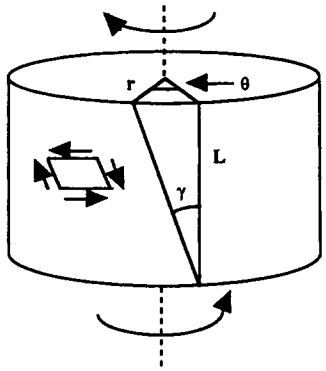

Figure 2 Diagram of torsion of a cylinder.

Table I Linear Density, Drawdown, and Tensile Properties of Polypropylene Yarns

Sample Number	Yarn Denier	Draw Ratio	Max Draw (%)	Tenacity (g/den)	Elongation (%)
pfc1	608.8	3.25	45	3.48	163
pfc4	623.2	4.72	66	4.67	30

Data are from Phillips Fiber Co.

$$\text{twist}_f = \frac{\phi f}{L_f} = \frac{2\pi(\text{no. revolutions fiber})}{L_f} \quad (4)$$

The torque at any distance r from the center of a cylinder is

$$dT = rdF \quad (5)$$

where T is the torque, F is the force, and r is the radial distance from the center. Because

$$dF = \tau dA \quad (6)$$

where τ is the shear stress and A is the area, we obtain

$$dT = \tau 2\pi r^2 dr \quad (7)$$

For a cylinder,

$$dT = \tau 2\pi \frac{\gamma^2}{\theta^2}\frac{dr}{\theta} \quad (8)$$

where $\gamma = r\theta$, the shear strain, $\theta = \phi/L$, the twist in radians per unit length (m^{-1}), and τ is the shear stress (Nm^{-2}). Integrating eq. (8) from the center of a filament of radius a to its outer surface where $\gamma = a\theta$, one obtains the general equation for torque in a cylinder,

$$T = \frac{2\pi}{\theta^3}\int_0^{a\theta} \gamma\tau(\gamma)\, d\gamma \quad (9)$$

For a linearly elastic material that obeys Hooke's law this reduces to eq. (2).

A torque–twist curve has the general shape of, and may be modeled with, the tangent function as

$$T = A\theta + B\tan^{-1}(C\theta) \quad (10)$$

Equating eqs. (9) and (10), after some relatively straightforward algebra one obtains

$$\tau(\gamma) = \frac{2A}{\pi a^4}\gamma + \frac{3B}{2\pi a^3}\tan^{-1}\left(\frac{C}{a}\gamma\right) + \left(\frac{BC}{2\pi a^4}\right)\left\{\frac{\gamma}{1 + (\gamma C/a)^2}\right\} \quad (11)$$

In general, the modulus is the derivative of the stress with respect to the strain. Thus, upon differentiating eq. (11) we get

$$G = \frac{2A}{\pi a^4} + \left(\frac{2BC}{\pi a^4}\right)\left\{\frac{\gamma}{1 + (\gamma C/a)^2}\right\} \quad (12)$$

Solving for the initial modulus at zero strain provides us with the modulus in terms of the measured radius and the parameters A, B, and C.

To determine the parameters A, B, and C, the model must be fit to the torque–twist data. This was accomplished by using a nonlinear fit routine in SAS®. Most of the torque–twist curves we obtained contained some degree of periodic oscillation. To obtain a better fit to the underlying curve, and therefore a more accurate determination of shear modulus, two sinusoidal terms were added to the model. The actual torque–twist data is extracted from the sinusoidal noise by the fitting process. The curve fitting process generates values for A, B, and C, as well as for the coefficients of the sinusoidal terms. Only the parameters A, B, and C are used in the calculation of the shear modulus.

Materials

Multifilament (612/34) PP yarn bundle samples were supplied by Phillips Fibers Corporation (now part of Amoco Corp.). The least drawn sample, pfc1, was produced on a spin–draw line; the other yarn, pfc4, was produced by a two-step process, spinning followed by drawing on a draw twist apparatus. The twist level was set at the minimum, and there was no noticeable twist in the filament bundle. Yarn data was supplied by Phillips Fiber Corporation (Table

I). The processing conditions for the yarns are listed in Table II.

Heat treatment of the pfc1 and pfc4 filaments was performed in order to modify their microstructures. Filaments were annealed either with fixed length, designated apfc, or with free ends, designated fpfc, in a 130°C oven for 1 h. For annealing at fixed length, the filament yarn, under a 100-g load, was wrapped on a metal frame. For the free end annealing, a length of yarn was cut and placed in a glass bowl. The bowl was placed in a 130°C oven for 1 h.

Test Methods

Tensile Testing

One-centimeter gage length samples of the filaments were tested on either the Instron Model 1125 or Model 4502 Mechanical Tester. The fibers were tested at a 50 mm/min crosshead speed. This testing rate was selected in order to cause plastic deformation of the fiber in approximately the same time as it occurred during torsion testing. The time period to break was usually between 7 and 15 s. Data was analyzed using the Materials Testing program. Load (kg), tenacity (g/den), percent elongation, and initial modulus (g/den) were calculated based on a gravimetric linear density measurement. The linear density measurement was necessary for the particular computer program linked to the Instron, but was subsequently removed in the conversion of tensile modulus from grams/denier to Newtons/square meter. Average cross-sectional areas were calculated from diameter measurements of approximately 50–65 filaments.

Birefringence

Fiber birefringence was determined using an aus-Jena® interference microscope. A filament in an immersion oil with $n = 1.510$ was covered with a glass coverslip and placed on the microscope stage. A camera linked the microscope to an Optimas® image analysis system. Refractive indices parallel and perpendicular to the fiber axis were determined using fringe shift measurements. Birefringence was calculated as $n_{\parallel} - n_{\perp}$.

Additionally, radial fringe shift scanning and quantification was performed on three filaments from each group at a separate facility.[46] The scanned images of the fringe shifts provided additional information to our birefringence studies.

Fiber Diameter

A nondestructive method for measurement of the fiber diameter d_f is by laser diffraction. The diameter of the fiber was calculated from

$$d_f = \frac{2\lambda}{\delta} \tag{13}$$

where δ is the distance between minima resulting from diffraction of the laser beam of wavelength λ around the fiber. This procedure was performed using a He-Ne laser with a wavelength of 632.8 nm, measuring the fringe spacing several times along the length of the fiber.

Torsion Testing

The fibers were mounted on 1-cm "c"-tabs and placed in the grips of the torsion test apparatus. Ten filaments were tested per set, for a total of four sets.

RESULTS

Fiber Diameter

Laser diffraction measurements of fiber diameter (Table III) revealed that the mean diameter of the pfc4 fibers was slightly larger than that of the pfc1 fibers. The apfc1 fibers showed a slight increase in

Table II Processing Parameters for Production of Polypropylene Yarns

Sample ID	Spin Process	Melt Temp. (°F)	Melt Pump Capacity (mL/rev)	Melt Pump Speed (rpm)	Feed Roll Speed (mpm)	Draw (%)	Roll Temp. *F/D/R* (°C)	Quench Temp. (°F)
pfc1	Spin–draw	510	2	38	165	320	85/95/95	72
pfc4	Spin, draw	510	2	42	124	472	25/85/105	72

Information provided by Phillips Fiber Corporation.

Table III Diameter, Linear Density, and Properties of As-Received and Annealed Polypropylene Filaments

Sample ID	Diameter (m)	Linear Density (den)	Tensile Modulus (g/den)	Tensile Modulus (N/m^2)	Tenacity (g/den)	Tenacity (N/m^2)	Elongation (%)
pfc1[a]	$5.40E-05$	18.15	13.59	$1.06E+09$	3.54	$2.75E+08$	227.8
	$(0.27E-05)$		(1.19)	$(0.09E+09)$	(0.193)	$(0.15E+08)$	(79.62)
pfc4[a]	$5.58E-05$	18.71	23.44	$1.77E+09$	4.958	$3.75E+08$	67.85
	$(0.31E-05)$		(2.25)	$(0.17E+09)$	(0.428)	$(0.32E+08)$	(50.29)
apfc1[b]	$5.57E-05$	18.15	15.48	$1.13E+09$	3.91	$2.86E+08$	160.1
	$(0.29E-5)$		(1.47)	$(0.11E+09)$	(0.189)	$(0.14E+08)$	(95.48)
apfc4[b]	$5.59E-04$	18.71	25.88	$1.94E+09$	5.534	$4.14E+08$	42.23
	$(0.30E-05)$		(1.93)	$(0.14E+09)$	(0.335)	$(0.25E+08)$	(1.74)
fpfc1[c]	$5.51E-05$	19.07	14.42	$1.13E+09$	3.595	$2.82E+08$	161.3
	$(0.29E-05)$		(1.63)	$(0.13E+09)$	(0.292)	$(0.23E+08)$	(103)
fpfc4[c]	$5.71E-05$	20.78	19.84	$1.58E+09$	4.885	$3.89E+08$	47.17
	$(0.22E-05)$		(1.37)	$(0.11E+09)$	(0.258)	$(0.21E+08)$	(1.77)

[a] See Tables I and II.
[b] Annealed at 130°C for 1 h at fixed length.
[c] Annealed at 130°C for 1 h with free ends.

mean diameter, while the mean diameter of the apfc4 fibers was unchanged from the untreated pfc4 filaments. The free end annealed filaments, fpfc1 and fpfc4, showed significant increases in diameter with respect to the as-received filament diameters.

Tensile Testing

Results of tensile testing of the fibers are shown in Table III. The pfc1 filaments had a much lower mean initial modulus than the pfc4 filaments. Moduli of both pfc1 and pfc4 filaments increased with annealing at a constant length, with the mean for apfc4 significantly higher than that for apfc1. Annealing with free ends resulted in a rise in the initial modulus for the fpfc1 filaments and a fall in the initial modulus for the pfc4 filaments.

Tenacity follows a similar pattern to the modulus (Table III). The mean value for the pfc1 filaments was lower than that of the pfc4 filaments. Tenacity values of both samples increased upon annealing at constant length. There was also a small increase in tenacity for both groups upon annealing with free ends.

Percent breaking elongation was higher for pfc1 than for pfc4 filaments (Table III). Coefficients of variance (%CV) were very large for both groups. Upon annealing at fixed length, percent elongation dropped for both apfc1 and apfc4. While %CV remained very high for apfc1, it dropped drastically for apfc4. Similarly, for fpfc1 percent elongation dropped but %CV was quite high, and for fpfc4 percent elongation dropped and the %CV was quite low.

Birefringence

Birefringence values for five fibers in each group are shown in Table IV. There was a statistically significant difference ($p < 0.05$) in birefringence between pfc1 and pfc4. Annealing at constant length resulted in a significant increase in birefringence in both apfc1 and apfc4. Free end annealed fibers fpfc1 and fpfc4 did not have significantly different birefringence than the as-received fibers. Both sets of heat

Table IV Birefringence Values for As-Received and Annealed Polypropylene Filaments

Sample ID[a]	Birefringence
pfc1	$2.88E-02$
	$(0.01E-02)$
pfc4	$3.15E-02$
	$(0.07E-02)$
apfc1	$3.14E-02$
	$(0.10E-02)$
apfc4	$3.26E-02$
	$(0.11E-02)$
fpfc1	$3.00E-02$
	$(0.06E-04)$
fpfc4	$3.14E-02$
	$(0.12E-03)$

[a] See Table III.

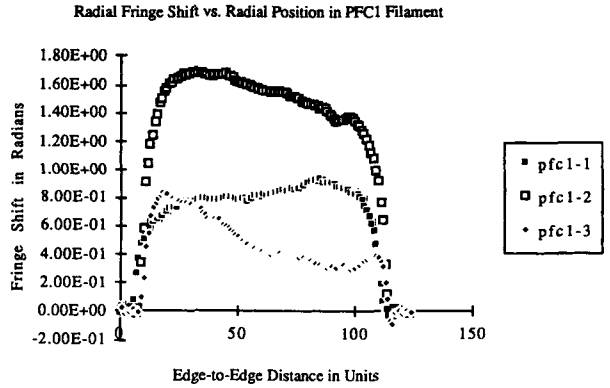

Figure 3 Radial parallel interference fringe shift for pfc1 filament.

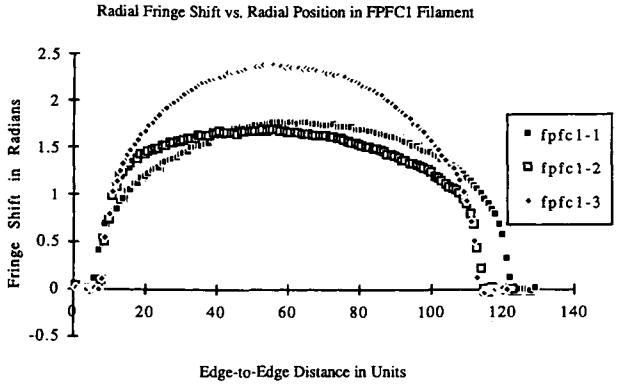

Figure 5 Radial parallel interference fringe shift for fpfc1 filament.

treated fibers did show significant differences in birefringence between the pfc1 and pfc4 filaments.

The parallel fringe shift data obtained for three fibers from each group are shown in Figures 3–8. There is an increase in the fringe shift upon annealing, which is greater for annealing at constant length than for annealing with free ends. There is a dip in the fringe shift for the pfc1 filament, which is indicative of differentiation in structure between the skin and the core of these filaments.

Torsion Testing

Shear moduli are presented in Table V. The mean values of the shear moduli were significantly ($p < 0.05$) greater for pfc4 than for pfc1, greater for apfc4 than for apfc1, and greater for fpfc4 than fpfc1, as illustrated in Figure 9. There was a significant difference in shear modulus between the annealed and the as-received fibers. The shear moduli of the fpfc4 filaments were lower than those of the apfc4 filaments, but the shear moduli are nearly identical for the fpfc1 and apfc1 filaments. Shear modulus appears to decrease with an increase in fiber diameter, both within a group, as for pfc1 (Fig. 10), and for all filaments, as in Figure 11.

DISCUSSION

Typically, in drawn PP filaments, an increase in draw ratio leads to increased initial extensional modulus. Both the initial as-spun structure of the filament and the conditions of drawing have a significant effect on the physical state of the filament during drawing and on the concomitant development of microstructure. Furthermore, it is commonly understood that quench conditions may induce a radial differentiation in microstructure. Subsequent thermal (annealing) and/or mechanical (drawing) treatments may exacerbate or exaggerate this difference in microstructure. Tensile modulus measurements are an average of properties across the filament and are therefore relatively insensitive to

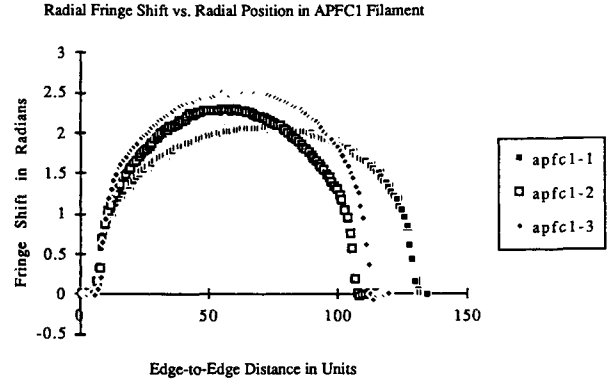

Figure 4 Radial parallel interference fringe shift for apfc1 filament.

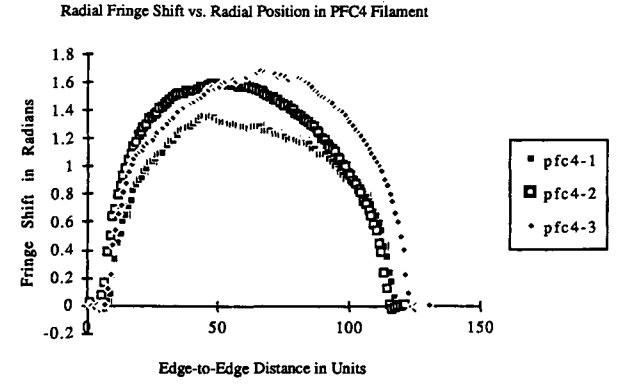

Figure 6 Radial parallel interference fringe shift for pfc4 filament.

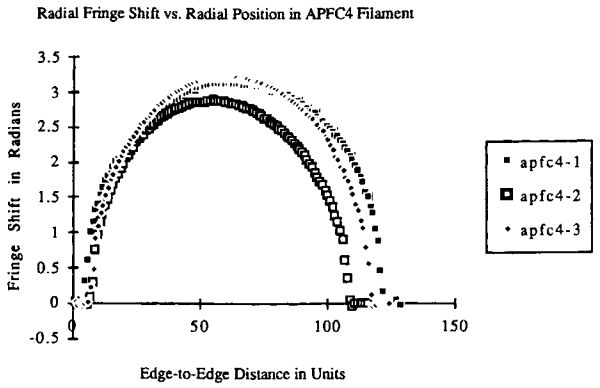

Figure 7 Radial parallel interference fringe shift for apfc4 filament.

any radial differentiation of structure. On the other hand, the nature of the torsional deformation makes it highly sensitive to such differences.

The effect of processing parameters on orientation and tensile properties may be explained by certain microstructural arguments. The increase in tensile modulus and overall birefringence between the as-received filaments, pfc1 and pfc4, indicate that the (drawn) pfc4 is the more highly oriented filament. Throughput was lower and take-up speed higher for the pfc1 filaments than for the pfc4 filaments, resulting in higher levels of spinline stress and more rapid drawdown for the pfc1 filaments. Thus, overall orientation would have been higher for the as-spun pfc1 filament than it was for the as-spun pfc4 filament. We presume a major effect of rapid cooling of filaments in the threadline to be a radial temperature gradient in the molten filament. This would result in a more highly crystalline but less oriented core. This effect would be more significant for the pfc1 filament than for the pfc4 filament. In fact, the dip in the radial refractive index profile for pfc1 (Fig. 3) is indicative of such a skin–core effect. Lower levels of spinline stress during production of the pfc4 filament would result in that material having a more uniform radial structure. It is important to note that after annealing, there is no indication of a skin–core differentiation in these materials (Figs. 4–8).

Because pfc1 filaments experienced a higher cooling rate than did pfc4, they could conceivably have a lower total crystallinity; and, with the concurrent increase in spinline stress, they could have smaller, more numerous crystallites and a higher number of interlamellar tie molecules. It seems reasonable, then, that the larger crystalline regions in the pfc4 filaments will have undergone a higher degree of destruction during the draw process than would the smaller crystalline regions in the pfc1 filaments; these smaller crystalline regions would deform more uniformly.[47] Micronecking of the large lamellar crystallites of pfc4 would result in strong elongated microfibrils, and a large number of taut inter- and intrafibrillar tie molecules within and among microfibrils, thus imparting the observed higher strength in the draw direction for the pfc4 filaments than for the pfc1 filaments. Although the as-spun pfc1 material may be more highly oriented, the orientation that occurred as a result of drawing was not high enough to cause a modulus above that of the pfc4 filaments. Hence, upon annealing with free ends, the pfc4 filaments, whose orientation was primarily developed through the destructive transformation to microfibrillar formation in drawing, would likely be more susceptible to shrinkage and return to its as-spun structure than would the pfc1 filaments, which had a more highly oriented as-spun structure, and a less dramatic transformation into their final microstructure. Indeed, the tensile data shows a significant decrease in tensile modulus of pfc4 upon annealing with free ends as compared with the anomalous slight increase in tensile modulus for pfc1 annealed under the same conditions (Table III). It is very unlikely that heat treatment with free ends would yield a more oriented fiber, so the presumed increase in tensile modulus for pfc1 must in some part be due to an increase in crystallite size and perfection.[34]

Upon annealing at constant length, an increase in tensile modulus for both the pfc1 and pfc4 filaments occurs (Table III). The birefringence values for both filament groups increases as well (Table IV). The mechanism for relaxation in annealing at constant length is by tie chain pullout.[36] An increase in tensile modulus under such conditions was explained by Peterlin to have occurred as a result of

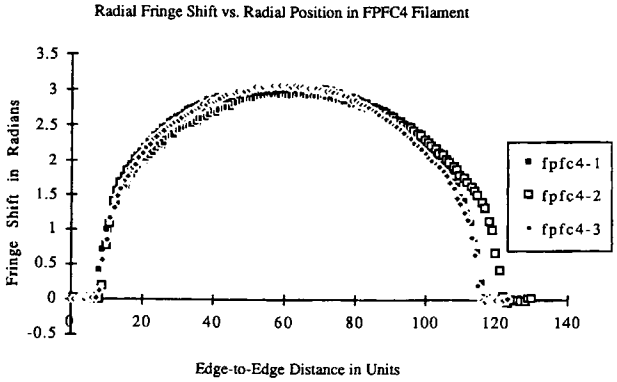

Figure 8 Radial parallel interference fringe shift for fpfc4 filament.

Table V Shear Moduli and Ratio of Tensile to Shear Moduli of As-Received and Annealed Polypropylene Filaments

Sample ID	Shear Mod. Set (N/m^2)					Average Shear Mod. (N/m^2)	Tensile Mod./Shear Mod.
	1	2	3	4	5		
pfc1	3.07E + 08	2.48E + 08	2.32E + 08	2.31E + 08	2.72E + 08	2.58E + 08	4.11
	(8.45E + 07)	(4.11E + 07)	(2.99E + 07)	(4.22E + 07)	(4.56E + 07)	(4.84E + 07)	
pfc4	2.71E + 08	2.92E + 08	3.15E + 08	2.88E + 08	3.07E + 08	2.95E + 08	6.01
	(4.92E + 07)	(4.04E + 07)	(4.00E + 07)	(2.52E + 07)	(3.53E + 07)	(3.83E + 07)	
apfc1	2.39E + 08	1.91E + 08	2.22E + 08	1.94E + 08	2.00E + 08	2.09E + 08	5.40
	(4.81E + 07)	(3.96E + 07)	(3.40E + 07)	(4.22E + 07)	(2.56E + 07)	(3.79E + 07)	
apfc4	2.63E + 08	2.81E + 08	2.91E + 08	3.05E + 08	2.90E + 08	2.86E + 08	6.78
	(4.74E + 07)	(5.92E + 07)	(2.01E + 07)	(8.94E + 07)	(6.39E + 07)	(5.60E + 07)	
fpfc1	1.91E + 08	2.04E + 08	1.84E + 08	2.03E + 08	2.32E + 08	2.03E + 08	5.57
	(1.89E + 07)	(2.03E + 07)	(2.21E + 07)	(7.11E + 07)	(7.47E + 07)	(4.22E + 07)	
fpfc4	2.33E + 08	2.72E + 08	2.22E + 08	2.90E + 08	2.71E + 08	2.58E + 08	6.13
	(2.15E + 07)	(3.41E + 07)	(3.72E + 07)	(4.24E + 07)	(5.87E + 07)	(3.83E + 07)	

formation of crystalline bridges by tie molecules between adjacent microfibrils.[36] It is thought that the increase in birefringence for PP filaments annealed under tension increases due to an increase in crystallinity.[48] Because crystalline regions are inherently more birefringent than the noncrystalline regions, an increase in the volume fraction of crystallinity would in general result in an increase in overall birefringence.

Shear moduli values (Table V) were well within the range of, although generally lower than, values previously reported for PP fibers.[12,29] A major contributing factor to the variability in these measurements is in the determination of the filament radius, because the radius enters into the modulus calculation to the fourth power [eq. (12)]. It is likely that our laser diffraction method for measuring fiber diameters is more accurate and precise than methods used by our predecessors in this field. This may account for the systematic difference between our shear modulus values and those previously reported.

There appears to be an overall decrease in the shear modulus with an increase in filament radius, as shown in Figure 11. The derivation of shear modulus is rooted in continuum mechanics, with the normal presumption of material homogeneity. The filaments tested in this study are not homogeneous but are anisotropic. In particular, as we discussed earlier, pfc1 may be expected to possess a microstructure with more radial differentiation than that of pfc4 (Fig. 10).

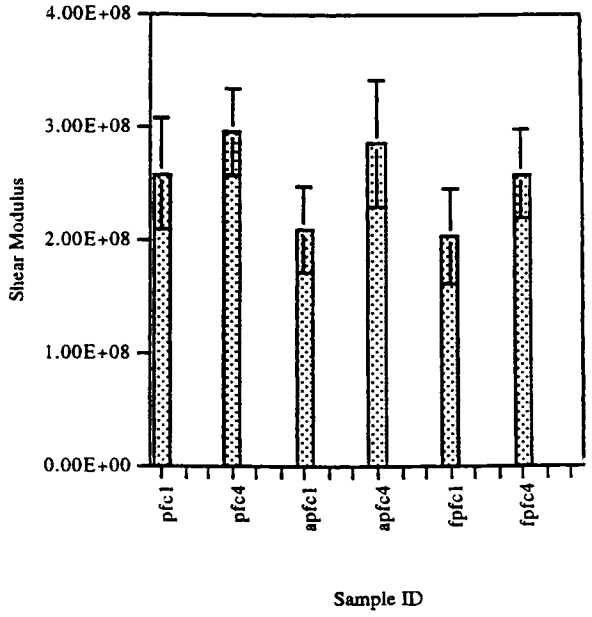

Figure 9 Shear moduli of polypropylene filaments.

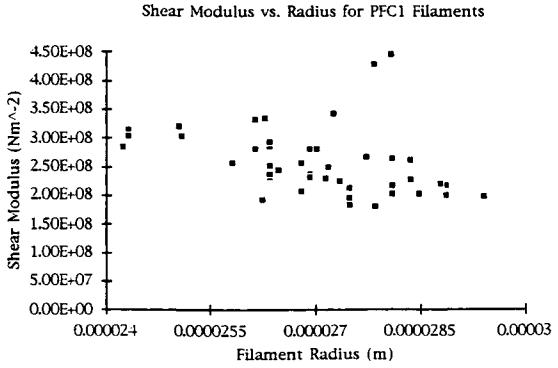

Figure 10 Shear moduli vs. radius for pfc1 filaments.

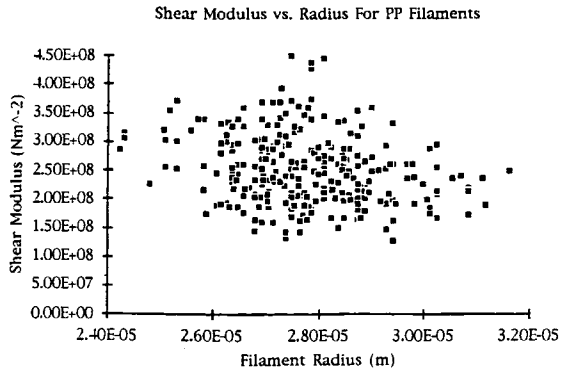

Figure 11 Shear moduli vs. radius for all polypropylene filaments.

In torsion, the fibrils and microfibrils experience shear stresses that cause them to slide over one another. For tie molecules embedded in crystallites in adjacent fibrils, the angle formed with respect to the transverse plane may determine the extent to which the molecule is strained in shear. For a positive twist, those molecules that form positive angles will become slack as fibrillar sliding occurs; those forming negative angles will experience high tensile stresses (Fig. 12). Therefore, only a fraction of the tie molecules contribute to the modulus, while others are not being strained. This would explain the difference in magnitude of the increase of the shear and tensile moduli with increasing orientation.

There are several possible effects of drawing and increased orientation on the shear modulus. In torsion, shear forces act both parallel to the fiber axis and in the transverse plane. In a drawn fiber, the typical mode of shear failure is by longitudinal splitting. This implies that at least a component of the shear stress acts longitudinally. The longitudinal shear modulus is lower than the transverse shear modulus, due to the axial fibrillation in the draw direction. For shear forces in the axial direction, the relationship of the shear modulus to the tensile modulus is due to the high degree of taut tie molecule orientation. At high draw ratios, the elongation and stretching of the interfibrillar taut tie molecules coupled with microfibrillar diameter reduction causes crystalline blocks in adjacent fibrils and microfibrils to be pulled more closely together, allowing van der Waal's bonding between adjacent segments to increase.[35] In addition, from a thermodynamic point of view, there are fewer degrees of freedom as the tie molecules are forced into an elongated state. From the standard presentations of statistical mechanics of polymers, this reduction in degrees of freedom results in an increase in modulus.[49]

At low draw ratios, the angles between tie molecules and the transverse normal to the fiber axis are larger, and fewer tie molecules would contribute to the shear modulus. Additionally, the microfibrillar structure is not fully developed, and portions of the original as-spun crystalline material remain in the filament. If the lamellae are oriented primarily parallel to the fiber axes, the interlamellar planes are subjected to transverse shear during torsion. It is likely that the shear modulus we measured is the interlamellar shear modulus, because the longitudinal component of shear was parallel to the longitudinal axes of the microfibrils, and the shear modulus in this direction is probably higher.

The effect on the shear modulus of annealing with free ends is a decrease in shear modulus, as expected, due to the decrease in orientation, and the reduction in the number of taut tie molecules. For fibers annealed at constant length, however, the effect is more complicated. While the shear modulus for pfc1 dropped, the shear modulus remained unchanged for pfc4. Additionally, there was an increase in tensile modulus for both filaments. If crystalline bridge formation between adjacent fibrils and microfibrils is responsible for the increase in tensile modulus, the shear modulus should be affected in the same manner.

One explanation for this departure from expected behavior is that, while the tensile strain is distributed evenly over the fiber cross-sectional area, the shear strain on a filament in torsion is greatest on the surface. Hence, the shear modulus is biased toward the modulus of the outer surface material. Upon annealing at constant length, the highly oriented skin material may relax around the core material, which would bear the tensile stress associated with the heat treatment. The pfc1 filament, which we would expect to have a higher proportion of skin

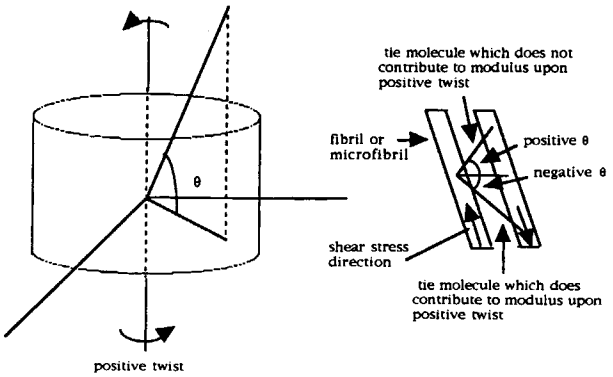

Figure 12 Schematic model of shear of a polypropylene filament.

to core material, would show a greater shear modulus drop upon annealing than would the pfc4 filaments. This was indeed the case.

In light of the sensitivity of the shear modulus to the microstructure of the outer portion of the filament, it is clear that use of the ratio of E/G as a measure of anisotropy may be misleading. The increase in E/G for free annealed pfc1 and pfc4 clearly illustrates this quandary (Table V).

CONCLUSION

We developed a computerized instrument capable of obtaining single filament torsion modulus data over a broad range of experimental conditions. The next iteration of this instrument is currently under development. We applied our instrument in an investigation of the relationship between the shear modulus and orientation of PP filaments. Shear modulus appeared to be related to orientation in the filament microstructure. While shear modulus increased with an increase in orientation, the increase was much less pronounced than the increase in the tensile modulus for the same change in orientation.

Although shear modulus as measured in torsion may not be the best indicator of amorphous orientation in a filament, our analysis implied it to be especially sensitive to the radial differentiation in the microstructure of the filament; in particular, the surface layers of a fiber would have the dominant effect on measured values of the torsional properties. This is presumably a result of the radial strain gradient produced by the torsional deformation of a cylinder. The mathematical model relating measured torque and torsion to the shear modulus is based on continuum mechanics, so presumptions of small deformations apply. Thus, we limited ourselves to calculation of initial modulus, i.e., small strain levels.

Some of the filaments investigated in this study showed evidence of radial microstructural variation. The shear moduli of these filaments was significantly reduced upon annealing at constant length, while the tensile modulus was slightly increased. It was proposed that the primary effect of the annealing process on these skin–core filaments was on the surface layers of the filaments. The effect on shear modulus of a radial structural variation will be the object of further study.

The authors wish to acknowledge the financial support of the School of Textile, Fiber, and Polymer Science of Clemson University, and, in the later stages of the work, the National Textile Center, a university research consortium.

REFERENCES

1. F. T. Peirce, *J. Textile Inst.*, **14,** T390–T413.
2. S. J. DeTeresa, R. S. Porter, and R. J. Farris, *J. Mater. Sci.*, **23,** 1886 (1988).
3. R. D. Adams and D. H. Lloyd, *J. Phys. E: Sci. Inst.*, **8,** 475 (1975).
4. H. Aghili-Kermani, T. O'Brien, D. D. Armeniades, and J. M. Roberts, *J. Phys. E: Sci. Inst.*, **9,** 887 (1976).
5. J. B. Enns and J. K. Gillham, in *Computer Applications in Applied Polymer Science,* T. Provder, Ed., American Chemical Society, Washington, D.C., 1982.
6. J. K. Gillham, *Org. Coatings Plast. Chem. Prepr.*, **44,** 503 (1981).
7. A. C. Goodings, *Textile Res. J.*, **38,** 123 (1968).
8. J. C. Guthrie, D. H. Morton, and P. H. Oliver, *J. Textile Inst.*, **45,** T912 (1954).
9. M. Karrholm, G. Nordhammar, and O. Friberg, *Textile Res. J.*, **25,** 922 (1955).
10. R. Meredith, *J. Textile Inst.*, **45,** T489 (1954).
11. R. Meredith, *J. Textile Inst.*, **48,** T163 (1957).
12. J. D. Owen, *J. Textile Inst.*, **56,** T329 (1965).
13. D. G. Phillips, *Textile Res. J.*, **57,** 415 (1987).
14. P. Z. Xiang, I. Ansari, and G. Pritchard, *Polym. Testing,* **5,** 321 (1985).
15. J. H. Wakelin, E. T. L. Voong, D. J. Montgomery, and J. H. Dusenbury, *J. Appl. Phys.*, **26,** 786 (1955).
16. P. Nordon, *J. Sci. Inst.*, **38,** 349 (1961).
17. P. Nordon, *Textile Res. J.*, **32,** 560 (1962).
18. L. D. Armstrong and M. Feughelman, *Textile Res. J.*, **39,** 261 (1969).
19. R. C. Dhingra and R. Postle, *J. Textile Inst.*, **65,** T126 (1974).
20. R. C. Dhingra and R. Postle, *J. Textile Inst.*, **65,** T171 (1974).
21. S. Kawabata, 4th Jpn.–U.S. Conf. Composite Mater., Washington, D.C., June 27–29, 1988.
22. W. F. Knoff, *J. Mater. Sci. Lett.*, **6,** 1392 (1987).
23. J. J. Mertens, *J. Textile Inst.*, **50,** T70 (1959).
24. W. E. Morton and F. Permanyer, *J. Textile Inst.*, **38,** T54 (1947).
25. W. E. Morton and F. Permanyer, *J. Textile Inst.*, **40,** T371 (1949).
26. M. Okabayashi and C. Yamazaki, *Textile Res. J.*, **46,** 429 (1976).
27. J. Skelton, *J. Textile Inst.*, **56,** T443 (1965).
28. R. L. Steinberger, *Textile Res.*, **7,** 83 (1936–1937).
29. D. W. Hadley, P. R. Pinnock, and I. M. Ward, *J. Mater. Sci.*, **4,** 152 (1969).
30. S. H. Zeronian, Q. Xie, G. Buschle-Diller, S. Holmes, and M. K. Inglesby, *J. Textile Inst.*, **85,** 293 (1994).
31. A. Peterlin, *J. Mater. Sci.*, **6,** 490 (1971).
32. J. E. Spruiell and J. L. White, *Polym. Eng. Sci.*, **15,** 660 (1975).

33. J. R. Dees and J. E. Spruiell, *J. Appl. Polym. Sci.*, **18,** 1053 (1974).
34. A. Ziabicki, *Fundamentals of Fiber Formation,* Wiley, New York, 1976.
35. K. Katayama, T. Amano, and K. Nakamura, *Kolloid Z.*, **226,** 125 (1968).
35. A. Peterlin, *Textile Res. J.*, **42,** 20 (1972).
36. A. Peterlin, *J. Appl. Phys.*, **48,** 4099 (1977).
37. H. Bodaghi, J. E. Spruiell, and J. L. White, *Int. Polym. Process.*, **III,** 100 (1988).
38. T. Kitao, J. E. Spruiell, and J. W. White, *Polym. Sci. Eng.*, **19,** 761 (1979).
39. H. P. Nadella, J. E. Spruiell, and J. L. White, *J. Appl. Polym. Sci.*, **22,** 3121 (1978).
40. R. J. Samuels, *J. Polym. Sci. Pt. A-2,* **6,** 2021 (1968).
41. G. M. Sze, J. E. Spruiell, and J. L. White, *J. Appl. Polym. Sci.*, **20,** 1823 (1976).
42. J. L. White, K. C. Dharod, and E. S. Clark, *J. Appl. Polym. Sci.*, **18,** 2539 (1974).
43. M. Ahmed, *Polypropylene Fibers—Science and Technology, Textile Science and Technology 5,* Society of Plastics Engineers, Inc., Elsevier, New York, 1982.
44. S. Timoshenko, *Strength of Materials Part 1, Elementary Theory and Problems,* 2nd ed., Van Nostrand, New York, 1940.
45. W. E. Morton and J. W. S. Hearle, *Physical Properties of Textile Fibres,* The Textile Institute, Manchester, U.K., 1962.
46. Z. Wu, Ph.D. Thesis, North Carolina State University, Raleigh, 1993.
47. A. O. Baranov and E. V. Prut, *J. Appl. Polym. Sci.*, **44,** 1557 (1992).
48. R. J. Samuels, *Structured Polymer Properties: The Identification, Interpretation, and Application of Crystalline Polymer Structure,* Wiley, New York, 1974.
49. J. Schultz, *Polymer Materials Science,* Prentice–Hall, Englewood Cliffs, NJ, 1974.

Received April 12, 1995
Accepted December 7, 1995